

Journal of Optoelectronical Nanostructures



Winter 2024 / Vol. 6, No. 1

Research Paper

Thin-film perovskite solar cell incorporating Gaussian and incremental gratings to optimize light absorption

Seyed Mohsen Mohebbi Nodez 1 , Masoud Jabbari 2 , Ghahraman Solookinejad 3 , Seyedeh Somayeh Mohebbi Nodez 4

- ¹ Department of Electrical Engineering, Bandar Abbas Branch, Islamic Azad University, Bandar Abbas, Iran.
- ² Department of Electrical Engineering, Marvdasht Branch, Islamic Azad University, Marvdasht, Iran.
- ³ Department of Physics, Marvdasht Branch, Islamic Azad University, Marvdasht, Iran.
- ⁴ Department of Electrical Engineering, Bandar Abbas Branch, Islamic Azad University, Bandar Abbas, Iran.

Received: Revised: Accepted: Published:

Use your device to scan and read the article online



DOI:

Abstract:

This paper proposes a Gaussian grating to enhance light absorption in perovskite thin-film solar cells. As gratings are effective structures for trapping light within the active layer of a cell, a two-dimensional Gaussian grating with a rectangular structure is considered for the front surface of the cell. Finite element method results demonstrate that the Gaussian grating significantly increases light absorption in a 0.5 micrometer thick cell within the visible and near-infrared range compared to a cell without a grating and a cell with a conventional or incremental grating. The average absorption of the cell with a Gaussian grating is 54.4%, representing a 68.33% increase compared to the

Citation: Seyed Mohsen Mohebbi Nodez, Masoud Jabbari, Ghahraman Solooki nejad, Seyedeh Somayeh Mohebbi Nodez. Thin-film perovskite solar cell incorporating Gaussian and incremental gratings to optimize light absorption. **Journal of Optoelectronical Nanostructures.** 2025; 1 (1): 48-58

Address: Department of Electrical Engineering, Marvdasht Branch, Islamic Azad University, Marvdasht, Iran. Tell: 00989177284080 Email: masoudjabbari@yahoo.com

^{*}Corresponding author: Masoud Jabbari

Keywords:

Thin-Film Solar Cells Perovskite, Gratings, Gaussian, Absorption, Plasmonic, Scattering. reference cell. Moreover, the short-circuit current density and efficiency were found to be 28.72 mA/cm² and 26.18%, respectively. The proposed cell structure shows promise for improved light-to-electricity conversion.



1. INTRODUCTION

Solar energy stands as a paramount source of clean, renewable, and ubiquitously accessible power, widely recognized as a key alternative energy vector globally. Despite the Sun's abundant irradiance, thin-film solar cells (SC) often exhibit suboptimal absorption rates, stemming from incomplete utilization of the solar spectrum [1, 2]. The current generation of solar cells predominantly relies on inorganic semiconductor materials, such as silicon. However, these materials entail substantial production costs and complex fabrication protocols [3]. Consequently, scientific inquiry has increasingly focused on the development of novel materials possessing the requisite characteristics for solar cell applications, while circumventing the limitations inherent in conventional inorganic photovoltaics. In this context, perovskites, a class of hybrid organic-inorganic materials, have garnered significant attention due to their advantageous properties, including remarkable flexibility, impact resilience, and facile processability [4–6]. Notable among their optoelectronic attributes are a tunable bandgap, a high absorption coefficient across a broad spectral range, and extended charge carrier diffusion lengths—on the order of one micron for electrons and several hundred nanometers for holes [7]. These extended diffusion lengths imply that photogenerated carriers can efficiently traverse considerable distances within the perovskite layer [8], making them highly suitable for thin-film solar cell architectures.Perovskite solar cells (PSCs) have demonstrated advancements in recent years, marked by substantial increases in power conversion efficiencies (PCEs). Researchers have reported a world-record PCE of 32.5% for perovskite tandem solar cells [9]. Strategies to enhance PSC performance have included the incorporation of randomly distributed plasmonic nanoparticles (NPs), which, through the excitation of surface plasmons, have been shown to boost photocurrents to levels such as 21.25 mA cm⁻² by using random Ag NPs [10]. Furthermore, recent developments have yielded PSCs with PCEs as high as 26.08%, attributed to meticulous control over perovskite layer crystallinity and surface morphology [11]. Nevertheless, a persistent challenge limiting the ultimate efficiency of PSCs remains their comparatively low light absorption. To augment solar cell (SC) efficiency, light-trapping methodologies are employed to enhance absorption [12]. These techniques encompass the utilization of nanostructures [13, 14], metallic nanoparticles [15], and grating architectures [16– 18]. Additionally, quantum mechanical phenomena such as intermediate bands [19] and hot carrier extraction [20] offer pathways to improve SC performance. Metallic nanostructures exhibit remarkable optical properties, capable of intensifying local electromagnetic fields through the excitation of localized surface plasmons (LSPs) and promoting light scattering, thereby attracting considerable research interest in recent years [21]. Grating nanostructures, characterized by periodic modulations in refractive index, induce variations in the phase, amplitude, or both properties of incident electromagnetic waves. This modification fundamentally alters wave behavior within the propagation medium, leading to phenomena such as light scattering and diffraction [22]. For instance, research in [23] proposed a dual-layer system of periodic graphene nanoribbons designed to achieve unidirectional plasmonically induced transparency (PIT) through an odd-to-even order resonance. The underlying principle relies on introducing a resonant phase difference between modes, which facilitates the PIT effect. In a separate study [24], single-layer rectangular graphene gratings were presented for achieving multi-band perfect plasmonic absorption. The mechanism driving this perfect absorption involves the excitation of standing-wave graphene surface plasmon polaritons (GSPPs). Notably, gratings with a bottom-open configuration enabled four-band perfect absorptions encompassing both even and odd order modes, whereas a continuous graphene sheet primarily supports evenorder modes. In the present work, plasmonic nanostructures integrated as backside gratings have been employed in the design of Perovskite Solar Cells (PSCs). Gratings positioned on the rear surface of the active layer facilitate the coupling of incident light to surface plasmon polaritons (SPPs) at the metal-dielectric interface, thereby enhancing light absorption within the active layer [25]. Several studies have explored strategies for absorption enhancement in PSCs. For example, silver nanoparticles were embedded within the active layer in [26] to boost absorption in the infrared region. These plasmonic effects were shown to generate high field intensities within the active layer, significantly improving light absorption, with an optimal condition yielding a 58.2% increase in infrared absorption. To mitigate optical losses and elevate the power conversion efficiency of PSCs, research in [27] utilized convex gratings for light trapping. In this configuration, incident light is concentrated within the active layer via scattering through surface plasmon resonances, consequently increasing absorption and leading to higher current density and efficiency. Similarly, a grating structure located on the backside of the active layer, as investigated in [28], enhances through light trapping and effectively suppresses carrier recombination. The designed SCs in this study demonstrated superior power conversion efficiency and optical current density compared to their reference counterparts. All proposed networks have a regular, periodic, or quasi-periodic structure that increases the absorption rate of the active layer. In this paper, a grating structure with a Gaussian distribution along the x-axis is presented and simulated using the finite element method (FEM). Gaussian gratings trap light by scattering it into the active layer, resulting in higher light absorption compared to solar cells with conventional gratings. The highest average absorption, short-circuit current density, and efficiency are 28.72 mA/cm², and 26.18%, respectively.

2. THE PROPOSED STRUCTURE

Figure 1 shows the schematic of the proposed solar cell with a Gaussian grating on its back surface. The proposed solar cell consists of a 250 nm thick silver back reflector, a 500 nm thick perovskite active layer, and a Gaussian distributed grating with width wg, height hg, and period P. The refractive indices of silver and perovskite are also taken from reference [26]. Equation (1) shows the distribution function used for the proposed Gaussian gratings, where prepresents the number of gratings, which is chosen as 9 in this paper, nave represents the average value of the gratings and is equal to 5, hg0 represents the height of the central grating, hg0 = 250 nm, and P0 is the period of the structure and is considered to be 300 nm, and ζ is also a constant that determines the width of the gratings. [27] In Figure 2, the Gaussian grating distribution is plotted for different values of ζ . It is observed that as the value of ζ increases from 0.2 to 0.7, the height of the side gratings increases. In order to achieve maximum absorption for all solar cells (SCs), the grating width and height were systematically varied across the proposed structures. The grating widths (wg) were considered in the range of 50-250 nm, while the heights were defined as h1=L×10 nm, h2=L×20 nm, $h3=L\times30$ nm, $h4=L\times40$ nm, and $h5=L\times50$ nm, where L=1,2,3,4,L=1,2,3,4, and 5. To investigate the effect of grating width and height on the SC performance, the average absorption as a function of hg was analyzed for different wg values. It was observed that increasing the grating dimensions leads to a reduction in the average absorption, exerting a negative impact on device performance. This phenomenon arises from the limited ability of such gratings to diffract and scatter light into the active layer. The reduction in absorption is further attributed to parasitic losses caused by metallic Ag nodes. To enhance light diffraction, an additional grating element with different dimensions was introduced adjacent to the initial grating, as illustrated in the SC configuration, resulting in improved absorption. The aim of this study was to determine the optimal grating width and height, and the configurations yielding the highest average absorption were identified as the most suitable structural parameters.

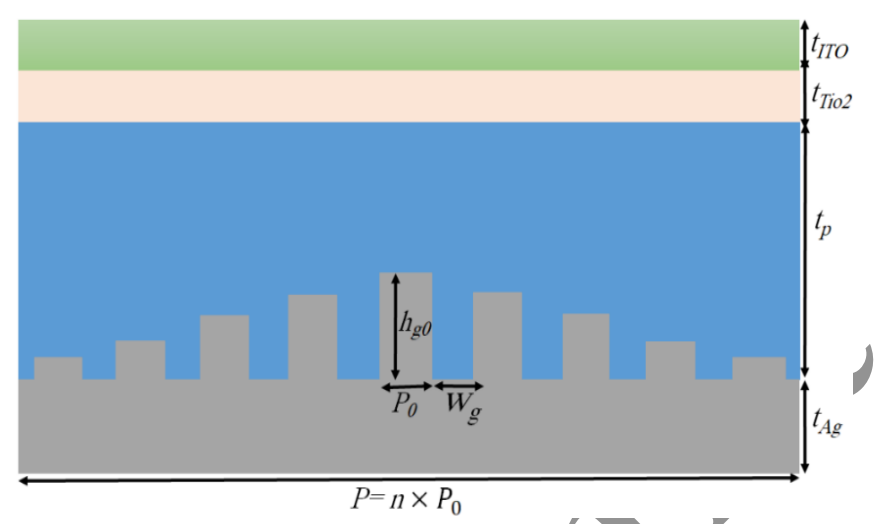
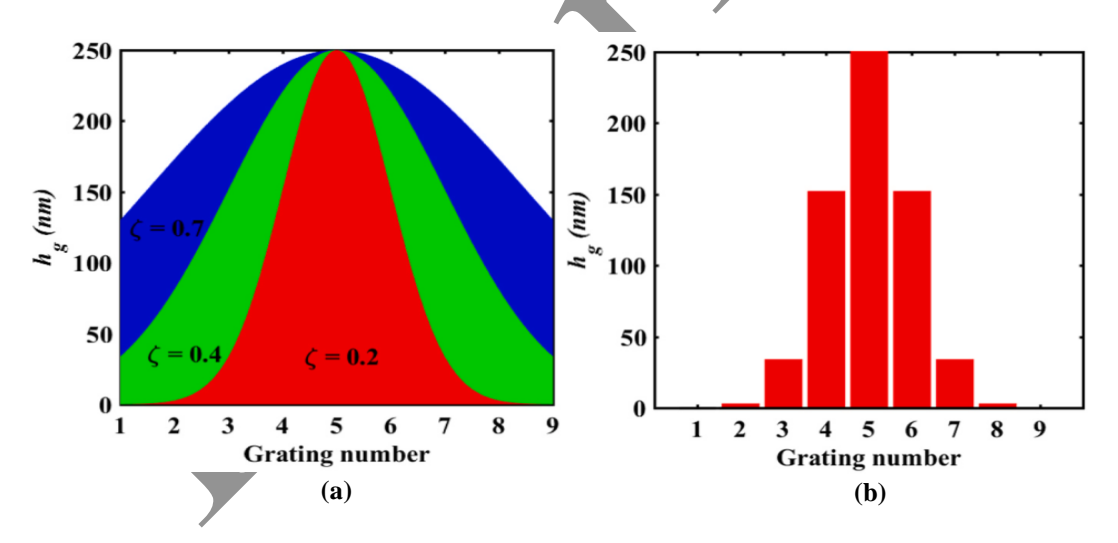


Fig. 1: Depiction of rear reflectors using a generalized Gaussian distribution for the development of an efficient light-trapping system.



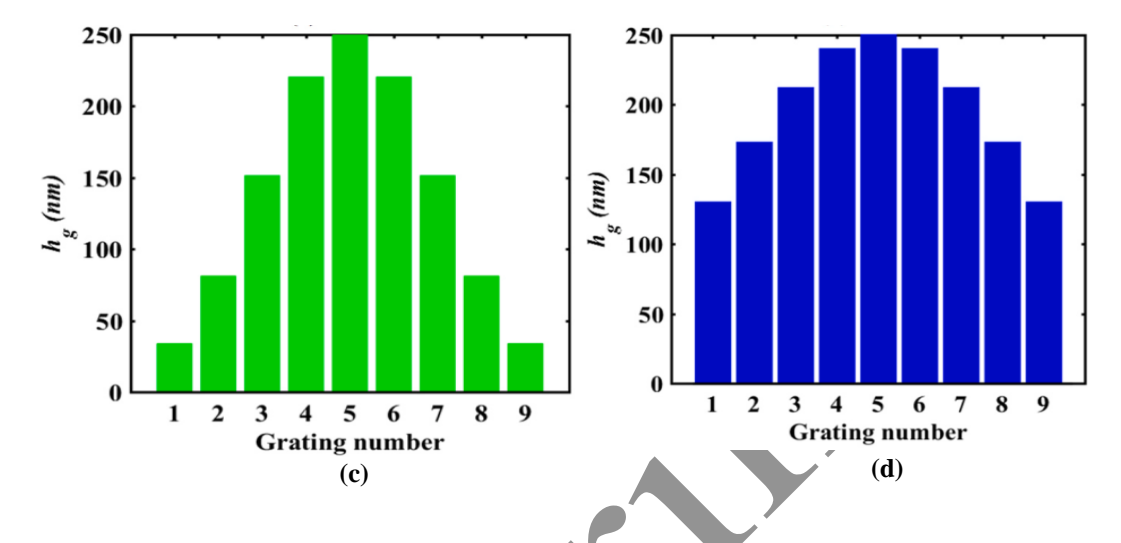


Fig. 2. a) Gaussian function distribution profile according to the number of gratings and for different ζ comprising of 0.1, 0.3, and 0.6; Gaussian grating distribution diagram are shown for: b) $\zeta = 0.1$, c) $\zeta = 0.3$ and d) $\zeta = 0.6$.

3. MATHEMATICAL FORMULATIONS

The figure shows how the parameter ζ affects the shape of the Gaussian curve and consequently the grating structure. A crucial parameter that plays a significant role in the design of solar cells is the plot of absorption versus the wavelength of incident light, which indicates the cell's ability to absorb light. Light absorption in each region of the cell can be calculated using equation (2) [27]:

$$h_g = h_{g0} exp \left(\frac{-\left(\frac{n}{n_{ave}} - 1\right)}{2\overline{\zeta}^2} \right)^2 \tag{1}$$

$$A(\lambda) = \frac{\varepsilon_0 \omega}{2} \frac{\varepsilon I''(\lambda)}{P_{in}(\lambda)} \int_{V} |E(\lambda)|^2 dV$$
 (2)

Where ω is the angular frequency, λ is the wavelength, $\epsilon 0$ is the permittivity of free space, $\epsilon(\lambda)$ is the imaginary part of the dielectric constant, $E(\lambda)$ is the wavelength-dependent electric field intensity, and $Pin(\lambda)$ is the solar irradiance. On the other hand, as a result of light irradiation, charge carriers are generated, which lead to the creation of a photocurrent, so that the short-circuit current

density and the open-circuit voltage of the cell can also be calculated from the following relations [27]:

$$J_{SC} = \frac{q}{hc} \int_{300nm}^{1000nm} \lambda A(\lambda) I(\lambda) d\lambda$$
 (3)

$$V_{OC} = \frac{KT}{q} ln \left(\frac{J_{ph}}{J_0} + 1 \right) \tag{4}$$

In this equation, q, h, c, λg , and $S(\lambda)$ represent the elementary charge, Planc constant, speed of light, perovskite bandgap wavelength, and solar radiation spectrum, respectively. Coupling is done in the wavelength domain λ min to λ max, as defined in reference [34]. A diffraction grating, A periodic structure refracts the incident light acts differen angle and acts as a scattering elemen separates the constituent wavelength of a light spectrum. The diffraction angle are determined by the incident angle (θ in), grating period (Δ), and wavelength landing light (λ), It is explained by the following equation [28]:

$$\theta_m = \sin^{-1}(\sin \theta_{in} + m\lambda/\Lambda); \quad |m| \le \Lambda/\lambda, \qquad m = 0, \pm 1, \pm 2, \dots$$
 (5)

By manipulating dimensions a diffuse grating, it thereby increases the absorption and absorption of light in the material.

$$\eta = \frac{J_{SC}V_{OC}FF}{P_{in}} \tag{6}$$

Where FF is the fill factor and Pin is the solar irradiance, which is equal to 100 milliwatts per square centimeter [27].

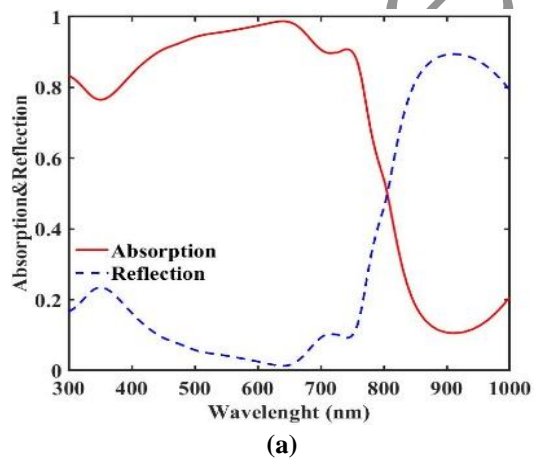
4. RESULT

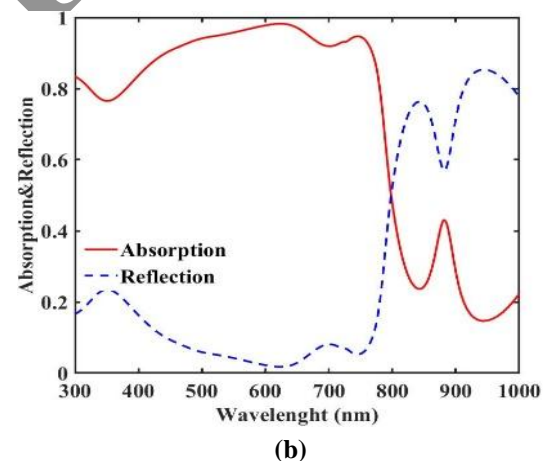
4.1.OPTIMAL DIMENSION

In this section, we present the simulation results of the proposed structure using the finite element method (FEM). Simulations include a cell without a grating (reference cell), cells with conventional and Gaussian gratings. In Figure 3, the absorption and reflection spectra of three types of solar cells with an active layer thickness of 500 nm are shown. Figure 3(a) corresponds to the reference cell, which has an average absorption of 47.5%. It is observed that this cell has a weak

absorption due to more light reflection from its surface. In this case, we observe absorption peaks at wavelengths of 743 nm and 883 nm. In order to increase its absorption, a conventional grating with a width and height of 100 nm and a period of 300 nm was used and its absorption spectrum is shown in Figure 3(b). It is observed that by applying the conventional grating, the amount of absorption in the visible region has increased significantly and the average absorption has reached 62.8%, which represents a 44.3% increase compared to the reference cell. The reason for this is the reduction of reflection from the cell surface and acting as an anti-reflection layer. The reason for the reduction in reflection is due to the scattering of light by the gratings. Thus, it can be concluded that by reducing the amount of reflection, more light scattering can be achieved in the active region, and as a result, absorption increases. In Figure 3(c), the amount of light absorption for hg0 = 250 nm, wg = 250 nm, and $\zeta = 0.3$ is plotted. It is observed that the presence of a Gaussian grating causes maximum light absorption in the visible wavelengths, and the average absorption reaches 54.4%, which represents a 68.33% increase compared to the reference cell. For a better comparison of the absorption spectra of the three types of cells, the absorption plot based on their

a 08.55% increase compared to the reference cent. For a better comparison of the absorption spectra of the three types of cells, the absorption plot based on their wavelength is shown in Figure 3(d). For the cell with Gaussian gratings, in addition to a significant increase in the visible region, we observe the formation of absorption peaks at longer wavelengths in the infrared region, which is due to the presence of gratings with different heights that scatter longer wavelengths into the active layer [29].





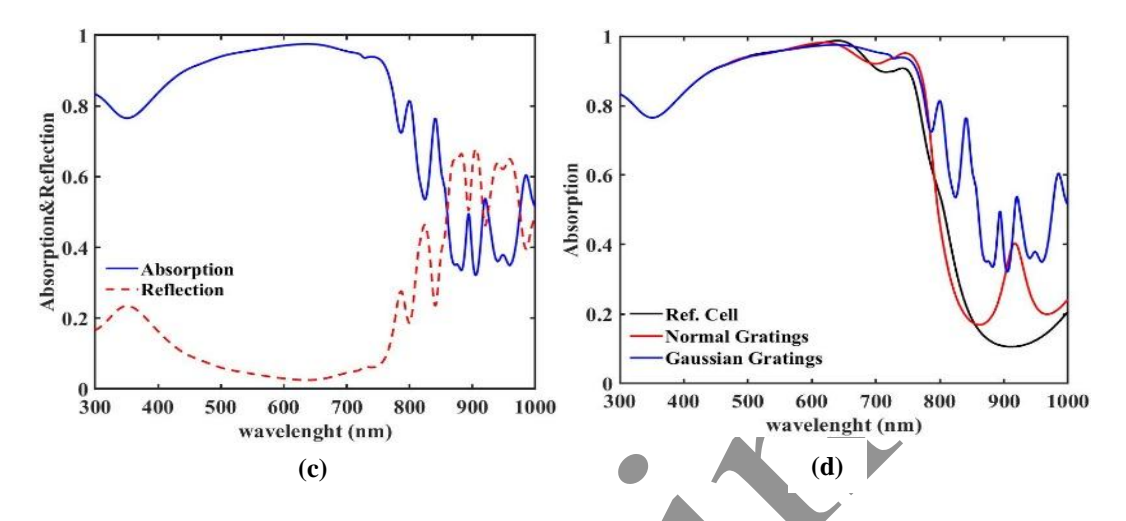


Fig. 3. Absorption and reflection spectra vs. wavelength for: a) reference cell, b) cell with normal gratings with wg = 100 nm, hg = 100 nm, and P0 = 300 nm, and c) cell with Gaussian grating for hg0 = 250 nm, wg = 250 nm, P0 = 300 nm, and $\zeta = 0.4$; d) Absorption spectra in terms of wavelength for all three types of SCs.

The reason for this is the reduction of reflection from the cell surface, acting as an anti-reflection layer. The decrease in reflection is due to the scattering of light by the gratings. Thus, it can be concluded that by reducing reflection, more light scattering can be achieved in the active region, leading to increased absorption. In Figure 3(c), the light absorption for hg0 = 250 nm, wg = 250 nm, and ζ = 0.3 is plotted. The presence of a Gaussian grating results in maximum light absorption in the visible wavelength range, with an average absorption reaching 85.6%, representing a 90% increase compared to the reference cell. For a better comparison of the absorption spectra of the three cell types, the absorption plot based on wavelength is shown in Figure 3(d). For the cell with Gaussian gratings, in addition to a significant increase in the visible region, absorption peaks are observed at longer wavelengths in the infrared region. This is due to the presence of gratings with varying heights that scatter longer wavelengths into the active layer [26]. where K and T indicate electron (hole) lifetime, Boltzmann constant, and temperature. The parameters used in the simulations are presented in Tab.1.

Table 1 Physical parameters of the layers used in the simulations.

Parameters	Compact TiO2	CH3NH3PbI3
Dielectric permittivity	10[29]	10[29]
Electron mobility (cm2/Vs)	100[29]	1.00[29]
Hole mobility (cm2/Vs)	25[29]	1.0[29]
Acceptor concentration (1/cm3)	0	1.0×1014[29]
Donor concentration (1/cm3)	1.0×1017[29]	0
Band gap (eV)	3.26[29]	1.5[29]
CB (1/cm3)	2.0×1017[29]	2.75×1018[29]
VB DOS (1/cm3)	6.0×1017[29]	3.9[29]
Affinity (eV)	4.2[29]	3.9[29]

In Table 2, the average absorption, short-circuit current density, and efficiency for all three types of cells are shown. It is observed that the short-circuit current density and efficiency increased from 21.6 mA/cm² and 11.8% in the reference cell to 24.37 mA/cm² and 15.4% in the cell with conventional gratings. Meanwhile, the values of current density and efficiency for the cell with Gaussian gratings are 28.72 mA/cm² and 26.18%, respectively.[26].

 $\begin{tabular}{ll} Table\ 2\\ Average\ absorption\ of\ the\ SC\ without\ grating\ and\ SCs\ with\ normal\ gratings\ and\ Gaussian\ gratings. \end{tabular}$

Gratings type	No	Normal	Gaussian
	gratings	gratings	gratings
Average absorption (%)	50.32	54.97	68.33
Short circuit current density (mA/cm2)	21.6	24.37	28.72
Efficiency (%)	22.35	22.31	26.18

The results indicate that increasing the grating size generally leads to a decrease in average absorption. This is attributed to the reduced efficiency of conventional gratings in scattering light into the cell, coupled with increased parasitic losses in silver gratings, which ultimately reduces net absorption. To enhance light scattering and absorption, Gaussian gratings with varying heights, widths, and ζ values, as described in [26], were introduced. Figures 4(b) and 4(a) show the average absorption for different widths and heights relative to different ζ values. The highest absorption is obtained at a width of 150 nm and a height of 250 nm for $\zeta = 0.3$.

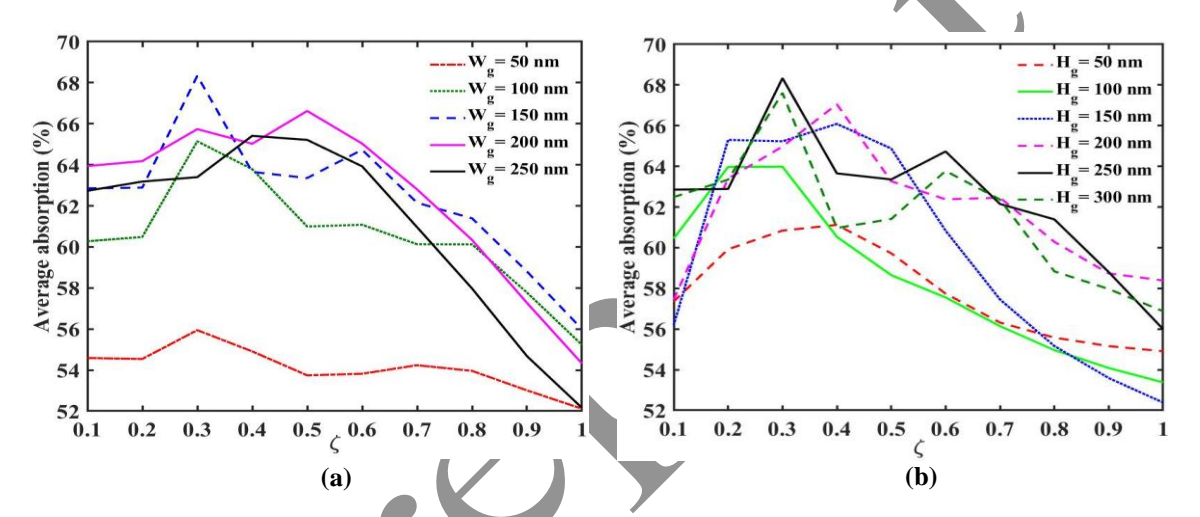


Figure .4. The average absorption versus hg with different wg for for SC the average absorption according to the ζ for different wg.

This section compares the findings of this research with similar studies, as presented in Table 2. Due to potential underestimation of losses in previous work, the comparison focuses on photocurrent derived the total absorption of perovskites layer. The results demonstrate that the proposd structure achieves the highst photocurent among compared devices. In [36,37], a study incorporated Al/SiO2 core-shell cluster nanoparticles within the perovskite layer. Their optimal configuration involved a 3 nm thick SiO2 shell, a central cluster NP with a 55 nm radius, and surrounding NPs with a 15 nm radius. In [38], another study used NPs with a 10 nm radius surrounded by 2 nm radius NPs. Compared to these approaches, the proposd structur offers a simpeler design while maintaining high performnces. Beyond Short circuit current, Efficiency, and Open circuit Voltage, additional crucial paramters for photovoltaic cells are photon absorption and

carier transport. In thin absorber, photon absorption is the dominant factor governing solar cell performance, whereas charge carrier transfer becomes more critical in thicker absorbers. In this research, the thin perovskite layer facilitates efficient charge carrier transport to the electrodes, minimizing the potential for carrier recombination within the layer. The enhanced photon absorption achieved through plasmonic effects is expected to translate into increased solar cell efficiency for the proposed structure, as supported by prior research [29,30].

Table 3
Short-circuit current density in this research and other similar researches

structure	Absorber thickness (nm)	A	Jsc (mA/cm ²)
This study	500		28.72
Al/SiO2 core-shell NPs [32]	250		22.28
lumpy Ag NPs[33]	50		22.05

Additionally, a comparison between the obtained results and those from experimental studies is presented in Table 3. Experimental data were obtained for a perovskite active layer thickness of 680 nm, a silver layer thickness of 250 nm, grating width of 214 nm.

Table 4
Short-circuit current density in this research and other similar researches

Absorber	Voc(mv)	Jsc (mA/cm ²)
thickness (nm)		
500	1100	28.72
500	1100	27.59
680	1160	23
680	1106	20.08
	thickness (nm) 500 500 680	thickness (nm) 500 1100 500 1100 680 1160

To gain a deeper understanding of light absorption enhancement phenomena, we conducted a physical analysis [26,34].

In Table 5, the effect of different temperatures, ranging from 270 to 350 K, on the solar cell structure has been investigated.

Table 5
Short-circuit current density in this research and other similar researches

Temperatures(K)	η (%)	Voc(v)	Jsc (mA/cm ²)
270	19.0	1.15	22
280	18.8	1.14	22.2
290	17.9	1.13	22.4
300	18.4	1.12	22.6
310	18.1	1.11	22.8
320	17.9	1.10	23.2
330	17.6	1.09	23.4
340	17.4	1.08	23.6
350	17.1	1.07	23.8

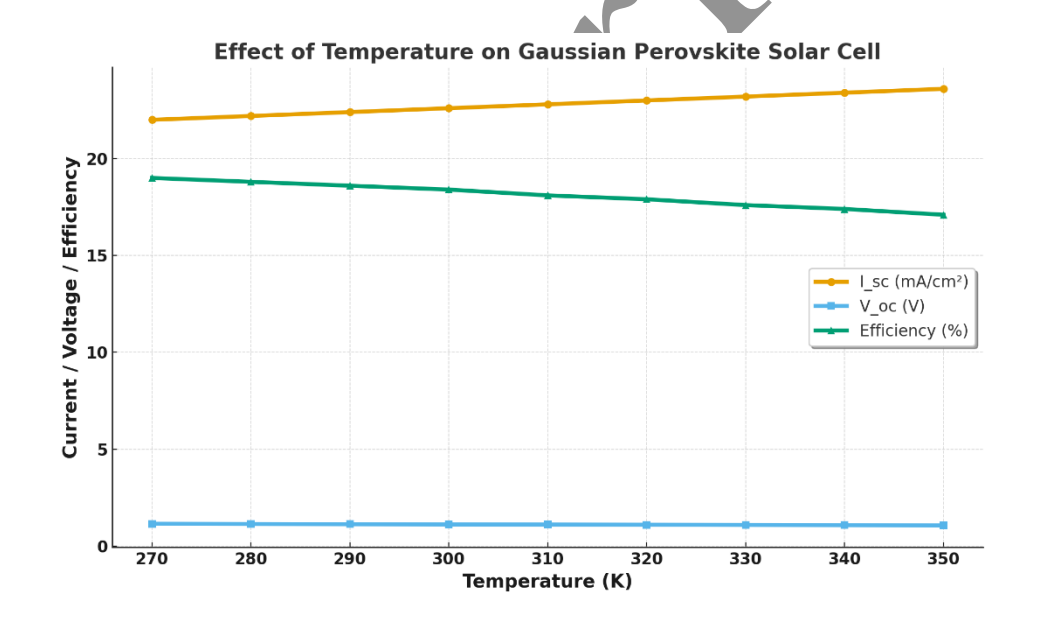


Fig.5. Effect of Temperature on Gaussian Perovskite Solar Cell.

To investigate the absorption mechanism in the proposed solar cells, the electric field intensity for the reference cell and cells with conventional and Gaussian gratings is shown in Figure 6. Figure 6-a shows the electric field intensity for the

reference cell at a wavelength of 741 nm, corresponding to the absorption peak. It is observed that the electric field has a uniform distribution, and darker regions are formed due to resonances. Due to the effect of light on the back reflector and its reflection into the active layer, constructive interference with the incident wave is formed, and absorption increases. In Figures 6(b) and 5(c), the electric field distribution profiles for the cell with conventional gratings at a wavelength of 835 nm and the cell with Gaussian gratings at a wavelength of 923 nm are shown, respectively. It is observed that both gratings have changed the distribution of field profiles within the active regions and formed darker spots, indicating light confinement and increased electric field intensity. On the other hand, due to the dependence of absorption on it, absorption increases[28].

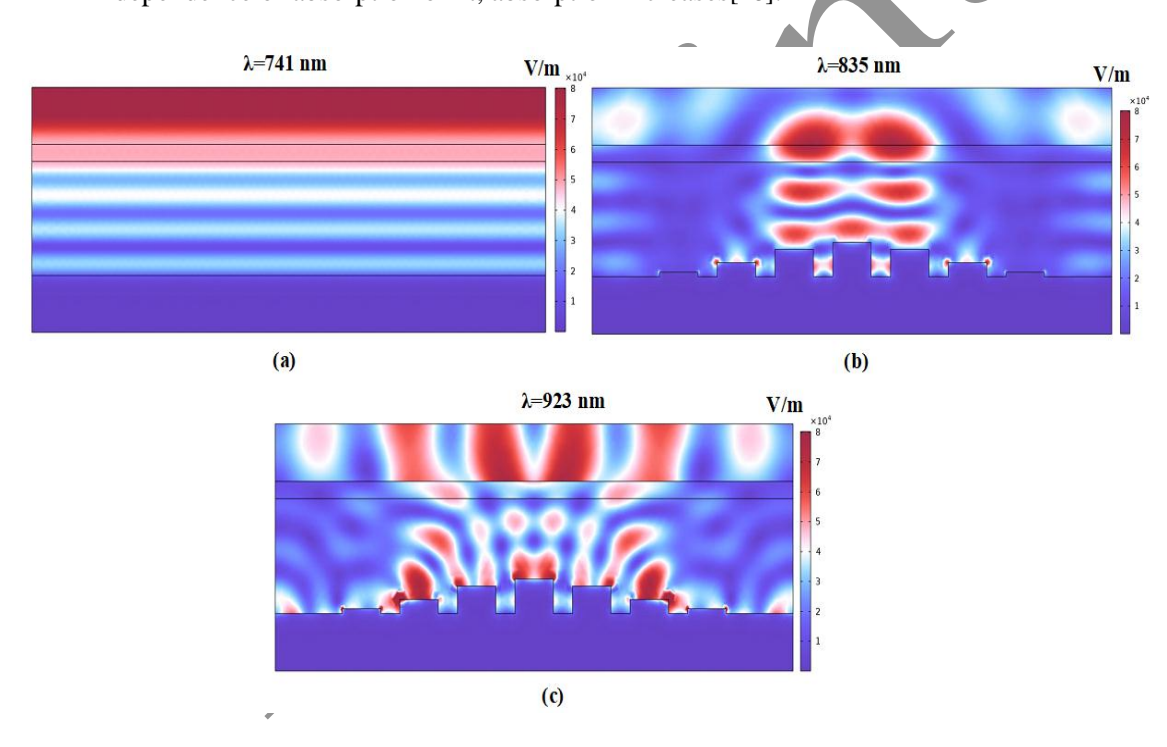
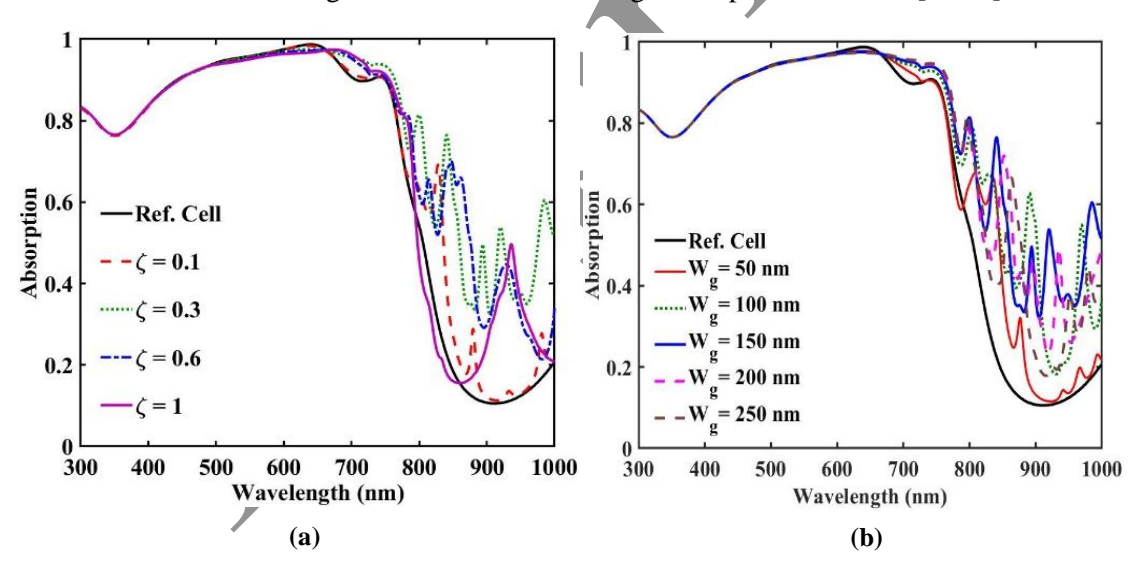


Fig.6. Electric field distribution profile for the: reference cell, b) cell with normal gratings and c) cell with Gaussian gratings at determined wavelengths.

In the following, we investigate the effect of parameters ζ , height hg0, and width wg in solar cells with Gaussian gratings. The absorption spectra as a function of wavelength for values of 0.1, 0.3, 0.6, and 1 are shown in Figure 7(a).

It is observed that when ζ is equal to 0.3, the absorption curve has the highest absorption value compared to the others. This is due to the ability to trap light by reducing light reflection from the cell surface, and it can be said that this height is the optimal dimension. To gain a physical insight into the mechanism of enhanced light absorption, the electric field intensity can be regarded as a key parameter of investigation. As expressed in Eqs. (2) and (3), the absorption is proportional to the square of the electric field intensity, and therefore can be improved with stronger field enhancement. Figure 6(a) illustrates the electric field distribution at the wavelength of 741 nm for the reference cell (Ref. Cell), corresponding to its absorption peak. As observed, the field in the reference structure is relatively uniform. In contrast, in the Gaussian SC, as shown in Figures 6(b) and 6(c), the electric field intensity at wavelengths of 835 nm and 923 nm is significantly enhanced due to the excitation of localized surface plasmons (LSPs) around the gratings. This plasmonic excitation not only increases the local field but also facilitates light scattering into the active layer, thereby extending the optical path length of photons, which enhances electronhole pair generation and improves the short-circuit current density. In this configuration, the electric fields between the back nodes are strongly amplified by LSP excitation, which results in more efficient light trapping within the active layer and consequently a higher density of photogenerated carriers. The gratings thus serve a dual role: trapping and scattering light within the active region, both of which contribute to improved absorption. Furthermore, the localized "hot spots" created by LSP excitation significantly increase the electric field intensity inside the active medium, leading to stronger carrier generation. Each grating produces a distinct resonance wavelength, which is highly sensitive to its geometric dimensions. As seen, the electric fields near the gratings at the rear side of the device are enhanced through LSP excitation. Since absorption is proportional to the square of the electric field, this enhancement directly translates into stronger absorption. In this case, the improvement in absorption primarily arises from prolonged photon trajectories within the active layer, which increases the probability of photon absorption and thereby enhances carrier generation and short-circuit current density. In Figure 7(b), the absorption spectra as a function of wavelength for different widths wg in the range of 50 to 250 nm are shown. In Figure 7(c), the effect of height hg0 on absorption is plotted. Gaussian gratings with a height of 250 nm show better absorption compared to other heights. In this paper, we focused on finding the optimal length, width, and height of the structure. Initially, we varied the width of the Gaussian grating structure from 0 to 300 nm, along with the height (different wg, hg, ζ) and period (PPP) between the gratings, to determine the most suitable structural width and height. After obtaining these optimal grating dimensions, our subsequent investigation aimed

to identify the specific height at which we observed maximum absorption peaks, plasmon excitation, enhanced electric fields, and the formation of 'hot spots' in the structure. Therefore, we first investigated the entire structure by keeping the width constant while varying the height, and then re-examined the structure with a constant height but varying widths. Based on the results of this systematic structural investigation, and considering the physical constraints on the height and width, we successfully determined the precise height and width that yielded the highest light absorption for this solar cell. It is observed that with increasing the width of the gratings, the absorption spectra show significant changes and their values increase, so that the highest absorption is observed at wg = 250 nm. The reason for this is the significant reduction in light reflection from the cell surface due to its scattering inside the cell. In other words, gratings with a width of 250 nm have the ability to couple more light into the active layer. In Figure 7(c), the average absorption spectrum as a function of ζ and for different heights hg0 is shown. It is observed that with increasing ζ from 0.1 to 1, the average absorption also increases, and at $\zeta = 0.3$, the highest average absorption of 85.6% is obtained. However, for values greater than 0.3, the average absorption decreases [26,29].



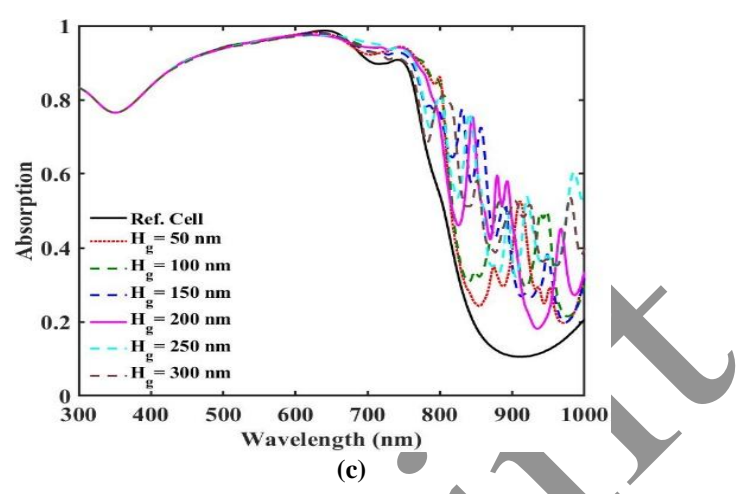
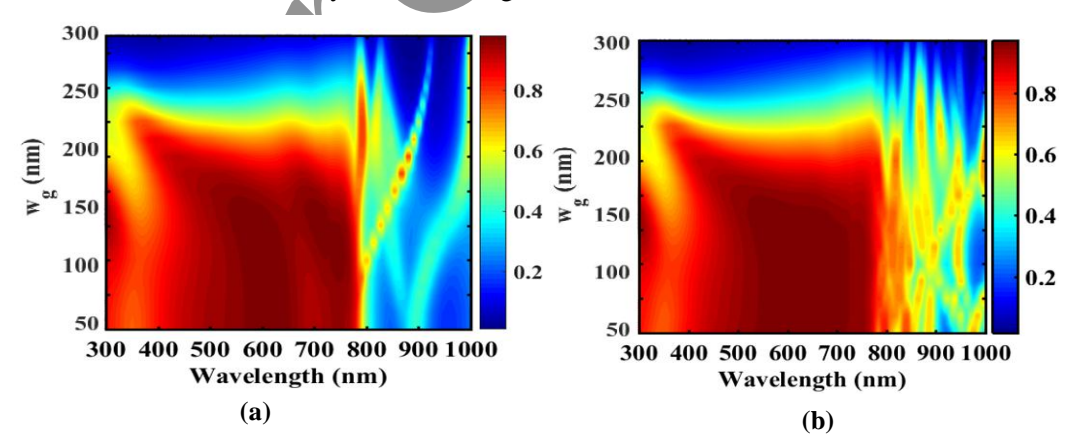


Fig. 7. Absorption spectrum in terms of wavelength for: a) different (c, b) differen

To investigate the effect of changing the grating width and ζ on absorption, all widths from 50 to 300 nm were swept, and the absorption spectra for $\zeta = 0.1$, $\zeta = 0.3$, and $\zeta = 1$ are shown in Figure 8. It is observed that the absorption value shows significant changes with variations in both width and ζ . This is because both parameters play an important role in reducing light reflection as an anti-reflection layer. Near-complete absorption occurred for $\zeta = 0.3$, which is better than the other two values, and an increase in absorption is observed for widths greater than 150 nm, as indicated by the darker regions [30,39].



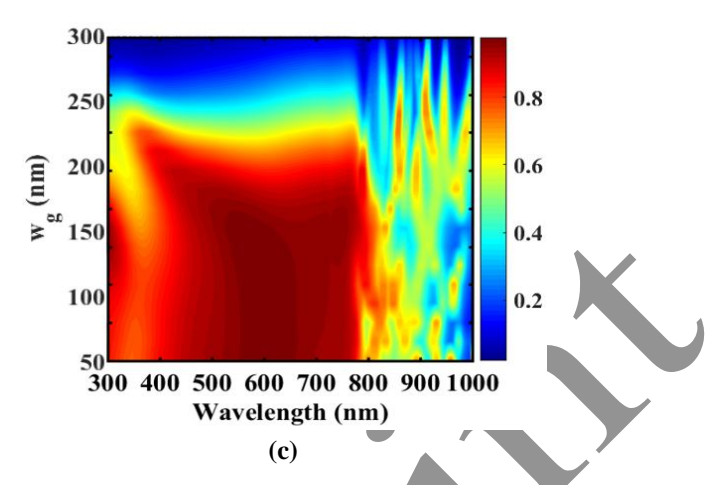


Fig. 8. Absorption spectra in terms of wavelength and gratings width for: a) $\zeta = 0.1$, b) $\zeta = 0.3$, and c) $\zeta = 1$.

4.2. Short-Circuit Current Density and Efficiency Analysis

Short-circuit current density and efficiency are two important parameters for analyzing the performance of solar cells. In Figures 9(a) and (b), the values of short-circuit current density and efficiency as a function of ζ for different hg0 values are shown, respectively. As can be seen, in each of the hg0 values, with increasing ζ, both current density and efficiency increase and reach a maximum value, and then show a decreasing trend. The reason for this is the changes in the amount of light absorption, since the current density is directly related to the absorbed light. The highest values of current density, 28.72 mA/cm², and efficiency, 26.18%, are obtained for $\zeta = 0.3$ and hg0 = 250 nm in Figure 8(a). In Figure 8(b), the effect of changing wg on both current density and efficiency is shown. In this case, $\zeta = 0.3$ and hg0 = 250 nm are selected, and it is observed that at wg = 250 nm, the maximum values of current density and efficiency occur. In Figure 9(c), the absorption spectrum as a function of wavelength and angle of incidence from 0 to 90 degrees for solar cells with Gaussian gratings is shown. It is observed that up to an angle of 45 degrees, the absorption for wavelengths less than 800 nm has values higher than 0.7, and therefore it can be said that Gaussian gratings perform well at oblique angles of incidence, and it is also clear in this figure that the Gaussian grating has an average of more than 78% for angles less than 40 degrees.

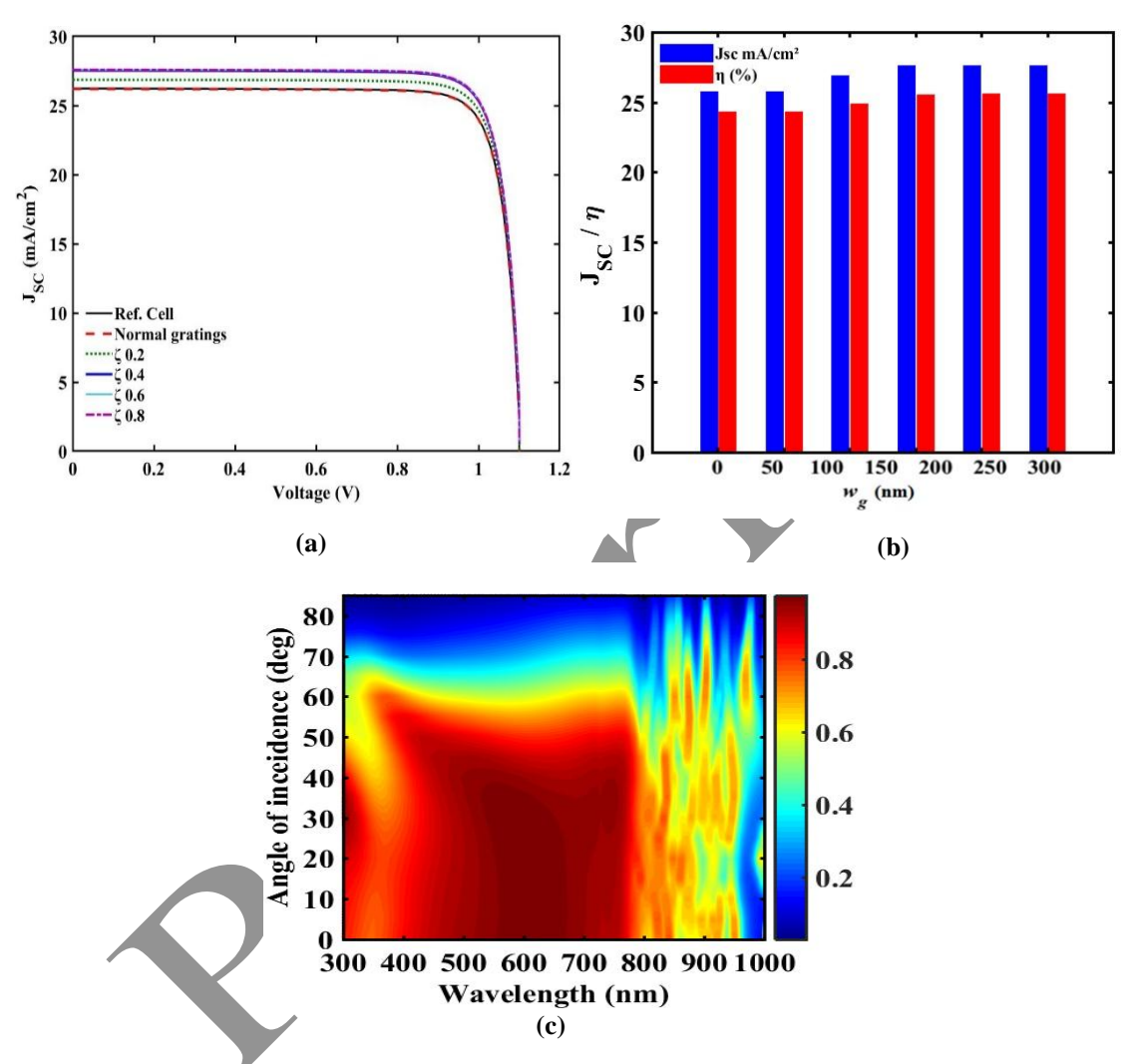


Fig. 9. a) Short circuit current density diagrams and efficiency in terms of grating width, and b) Current-voltage characteristic for reference cell, c) Absorption spectrum of cell with Gaussian gratings in terms of wavelength and radiation angle.

5.CONCLUSION

Due to their unique structure, gratings scatter light into the active region, thereby increasing light absorption. Various types of grating structures, including one-

dimensional and two-dimensional gratings with regular and random distributions, have been presented in different works. In this paper, the effect of Gaussian gratings on increasing absorption in the active layer of perovskite solar cells was investigated. To this end, Gaussian gratings were considered on the front surface of the cell, and the absorption rate in the active region was calculated and compared with the absorption rate of the reference cell and the cell with a conventional grating. FEM simulation results showed that these types of gratings, due to their special geometry, effectively trap sunlight within the active layer and significantly increase the amount of absorption in the visible and near-infrared regions of the solar spectrum. The findings show that the average absorption of cells with Gaussian gratings is 54.4%, which represents a 68.33% increase compared to the absorption of reference cells. On the other hand, the short-circuit current density and efficiency were obtained as 28.72 mA/cm² and 26.18%. Therefore, a newly designed perovskite solar cell with higher absorption and efficiency was presented, which is capable of converting more light into electricity.

References

- [1] E.R.W. Mac Queen, M. Liebhaber, J. Niederhausen, M. Mews, C. Gersmann, S. Jackle, K. Lips, *Crystalline silicon solar cells with tetracene interlayers: the path to siliconsinglet fission heterojunction devices*, Mater. Horiz. 5 (6) (2018) 1065–1075, Available: https://doi.org/10.1039/C8MH00853A
- [2] C. Battaglia, A. Cuevas, S.D. Wolf, *High-efficiency crystalline silicon solar cells status and perspectives*, Energy Environ. Sci. 9 (5) (2016) 1552–1576, Available: https://doi.org/10.1039/C5EE03380B
- [3] H. Naim, D.K. Shah, A. Bouadi, M.R. Siddiqui, M.S. Akhtar, C.Y. Kim, An in-depth optimization of thickness of base and emitter of ZnO/Si heterojunction-based crystalline silicon solar cell: a simulation method, J. Electron. Mater. 51 (2) (2022)586–593,Available: https://doi.org/10.1007/s11664-021-09341-5.
- [4] S. Cao, D. Yu, Y. Lin, C. Zhang, L. Lu, M. Yin, D. Li, *Light propagation in flexible thin-film amorphous silicon solar cells with nanotextured metal back reflectors*, ACS Appl. Mater. Interfaces 12 (23) (2020) 6184–26192, https://doi.org/10.1021/acsami.0c05330.
- [5] D.L. McGott, C.P. Muzzillo, C.L. Perkins, J.J. Berry, K. Zhu, J.N. Duenow, M.O. Reese, *3D/2D passivation as a secret to success for*

- polycrystalline thin-film solarcells, Joule 5 (5) (2021) 1057–1073, Available: https://doi.org/10.1016/j.joule.2021.03.015.
- [6] J. Ramanujam, D.M. Bishop, T.K. Todorov, O. Gunawan, J. Rath, R. Nekovei, A. Romeo, *Flexible CIGS*, *CdTe and a-Si: H based thin film solar cells: a review*, Prog. Mater. Sci. 110 (2020) 100619, Available: https://doi.org/10.1016/j.
- [7] X. Zhaopeng, H. Huangfu, L. He, J. Wang, D. Yang, J. Guo, H. Wang, Light-trapping properties of the Si inclined nanowire arrays, Opt. Commun. 382 (2017) 332–336, Available: https://doi.org/10.1016/j.optcom.2016.08.018.
- [8] M.A. Elrabiaey, M. Hussein, M.F.O. Hameed, S.S. Obayya, *Light absorption enhancement in ultrathin film solar cell with embedded dielectric nanowires*, Sci. Rep. 10 (1) (2020) 17534, Available: https://doi.org/10.1038/s41598-020-74453-7.
- [9] R. Ren, Z. Zhong, Enhanced light absorption of silicon solar cells with dielectric nanostructured back reflector, Opt. Commun. 417 (2018) 110–114, Available:https://doi.org/10.1016/j.optcom.2018.02.051.
- [10] Y.H. Jang, Y.J. Jang, S. Kim, L.N. Quan, K. Chung, D.H. Kim, *Plasmonic solar cells: from rational design to mechanism overview*, Chem. Rev. 116 (24) (2016)14982–15034, Available: https://doi.org/10.1021/acs.chemrev.6b00302.
- [11] F. Enrichi, A. Quandt, G.C. Righini, *Plasmonic enhanced solar cells:* summary of possible strategies and recent results, Renew. Sustain. Energy Rev. 82 (2018) 2433–2439, Available https://doi.org/10.1016/j.rser.2017.08.094
- [12] L. Long, Y. Yang, L. Wang, Simultaneously enhanced solar absorption and radiative cooling with thin silica micro-grating coatings for silicon solar cells, Sol. Energy Mater. Sol. Cell 197 (2019) 19–24, Available: https://doi.org/10.1016/j.solmat.2019.04.006.
- [13] T. Sun, H. Shi, L. Cao, Y. Liu, J. Tu, M. Lu, F. Zhang, *Double grating high efficiency nanostructured silicon-based ultra-thin solar cells*, Results Phys. 19(2020)103442, Available: https://doi.org/10.1016/j.rinp.2020.103442.
- [14] C. Heine, R.H. Morf, *Submicrometer gratings for solar energy applications*, Appl.Opt. 34 (14) (1995) 2476–2482, Available: https://doi.org/10.1364/AO.34.002476.

- [15] S. Elewa, B. Yousif, M.E.A. Abo-Elsoud, *Improving efficiency of perovskite solar cell using optimized front surface nanospheres grating*, Appl. Phys. A 127 (11)(2021) 1–14, Available:https://doi.org/10.1007/s00339-021-05019-1
- [16] P. Tillmann, B. Bl⁻ asi, S. Burger, M. Hammerschmidt, O. Hohn, ⁻ C. Becker, K. J⁻ ager, *Optimizing metal grating back reflectors for III-V-on-silicon multijunction solarcells*, Opt. Express 29 (14) (2021) 22517–22532, Available: https://doi.org/10.1364/OE.426761
- [17] R. Chen, Z. Hu, Y. Ye, J. Zhang, Z. Shi, Y. Hua, *An anti-reflective 1D rectangle grating on GaAs solar cell using one-step femtosecond laser fabrication*, Opt. Lasers Eng. 93 (2017) 109–113, Available: https://doi.org/10.1016/j.optlaseng.2017.01.017.
- [18] W. Lan, Y. Wang, J. Singh, F. Zhu, *Omnidirectional and broadband light absorption enhancement in 2-D photonic-structured organic solar cells*, ACS Photonics 5 (3)(2018) 1144–1150, Available:https://doi.org/10.1021/acsphotonics.7b01573.
- [19] A.P. Amalathas, M.M. Alkaisi, *Nanostructures for light trapping in thin film solar cells*, Micromachines 10 (9) (2019) 619, Available: https://doi.org/10.3390/mi10090619
- [20] K.X. Wang, Z. Yu, V. Liu, Y. Cui, S. Fan, Absorption enhancement in ultrathin crystalline silicon solar cells with antireflection and light-trapping nanocone gratings, Nano Lett. 12 (3) (2012) 1616–1619, Available:https://doi.org/10.1021/nl204550q.
- [21] H. Zheng, Y. Yu, R. Wu, S. Wu, S. Chen, K. Chen, *Period-mismatched sine dualinterface grating for optical absorption in silicon thin-film solar cells*, Applied Optics. 59 (33) (202) 10330–10338.

 Available:https://doi.org/10.1364/AO.408812.
- [22] K. Chen, N. Zheng, S. Wu, J. He, Y. Yu, H. Zheng, *Effective light trapping in c-Si thin-film solar cells with a dual-layer split grating*, Appl. Opt. 60 (33) (2021)10312–10321, Available: https://doi.org/10.1364/AO.443307.
- [23] J. Zhang, Z. Yu, Y. Liu, H. Chai, J. Hao, H. Ye, *Dual interface gratings design for absorption enhancement in thin crystalline silicon solar cells*, Opt. Commun. 399 (2017) 62–67, Available: https://doi.org/10.1016/j.optcom.2017.04.062.
- [24] Bozzola, M. Liscidini, L.C. Andreani, *Broadband light trapping with disordered photonic structures in thin-film silicon solar cells, Prog.* Photovolt.: Res. Appl. 22 Available: https://doi.org/10.1002/pip.2385.

- [25] Elshorbagy, M. H., Abdel-Hady, K., Kamal, H., & Alda, J. (2017). Broadband anti-reflection coating using dielectric Si3N4 nanostructures. Application to amorphous-Si-H solar cells. Optics Communications, Available: https://doi.org/10.1016/j.optcom.2016.12.06 2.
- [26] Mohebbi Nodez, S. M., Jabbari, M., & Solookinejad, G. (2023). Absorption enhancement of Perovskite Solar Cells using multiple Gratings. Physica Scripta. Available: https://doi.org/10.1088/1402-4896/ace2f6
- [27] Hamid Heidarzadeh (2019), Incident light management in a thin silicon solar cell using a twodimensional grating according a Gaussian distribution. Available: https://doi:10.1016/j.solener.2019.07.099.
- [28] E.G. Loewen, E. Popov, *Diffraction Gratings and Applications*, Journal of CRC Press, Available: https://doi:10.1201/9781315214849.
- [29] Mohammed.m,Hala J. El-Khozondar,Salah A.Nassar, Guillaume Zoppi, Yasser F. Nassar, *Design and optimization of plasmonic nanoparticles-enhanced perovskite solar cells using the FDTD method*, Journal of Solar energy.Available: https://doi:10.51646/jsesd.v13i1.170.
- [30] S. In, D.R. Mason, H. Lee, M. Jung, C. Lee, N. Park, Enhanced Light Trapping and Power Conversion Efficiency in Ultrathin Plasmonic Organic SolarCells, Journal of ACSPhotonics,
- Available: https://doi.org/10.1021/ph500268y.
- [31] HOSSAIN M I, ALHARBI F H, TABET N. Copper oxide as inorganic hole transport material for lead halide perovskite based solar cells[J]. Solar energy, 2015, 120-370-380.
- [32] B. Cai, Y. Peng, Y.-B. Cheng, M. Gu, 4-fold photocurrent enhancement in ultrathin nanoplasmonic perovskite solar cells, Journal of Opt. Express, OE. 23(2015)A1700–A1706.Available: https://doi.org/10.1364/OE.23.0A1700.
- [33] A. Jangjoy, S. Matloub, Optical simulation and design of highabsorption thin-film perovskite halide solar cells based on embedded quadrilateral cluster nanoparticles, Journal of Solar Energy.
- Available: https://doi: 10.1016/j.solener.2022.07.004.
- [34] Jiangang Feng, Xi Wang, Jia Li, Haoming Liang, Wen Wen3, Ezra Alvianto, Cheng-Wei Qiu, Rui Su & Yi Hou, *Resonant perovskite solar cells with extended band edge*. Journal of Nature Communications.
- Available: https://doi:10.1038/s41467-023-41149-1.
- [35] Seyed Nooreddin Jafari, Abbas Ghadimi, Saeed Rouhi, *Strained Carbon Nanotube (SCNT) Thin Layer Effect on GaAs Solar Cells Efficiency*. Journal of Optoelectronical Nanostructures.

Available: https://jopn.marvdasht.iau.ir/article_4505_8947f89a5f380e375d5e6425249c10b5.pdf

- [36] Marzieh Akbari, Fatemeh Dabbagh Kashani, Seyed Mohhammad Mir Kazemi, Enhancing CIGS Solar Cell Efficiency through Gold, Silver, and Aluminum Plasmonic Nanostructures. Journal of Optoelectronical Nanostructures. Available:https://doi.org/10.71577/jopn.2025.1207117.
- [37] Hasan Kanani, Saeed Golmohammadi, Hassan Rasooli Saghai, Jaber Pouladi, Light Absorption Improvement in Si Thin Film Solar Cells Using Combination of Graphene-based nanoparticle and strips-grooves geometry. Journal of Optoelectronical Nanostructures.

Available: https://doi.org/10.71577/jopn.2025.1187845

- [38] Seyed Mohsen Mohebbi Nodez, Masoud Jabbari, Ghahraman Solookinejad, *Light management in Peroyskite Solar Cells using multiple Gratings*. Journal of Optoelectronical Nanostructures. Available: https://doi.org/10.71577/jopn.2024.1182867.
- [39] Fereshte Bagheri, *Investigating factors affecting loss reduction in graphene-based plasmonic structures*, Journal of Optoelectronical Nanostructures. Available: https://doi.org/10.71577/jopn.2025.1210152

